RAPID COMMUNICATION

Optical study of charge dynamics in $CaCo_2As_2$*

Wei Zhang(张威)[1,2], Bing Xu(许兵)[2], Run Yang(杨润)[2],
Jin-Yun Liu(刘金云)[2], Hao Yang(杨浩)[3,†], and Xiang-Gang Qiu(邱祥冈)[2,‡]

[1] *College of Physics, Optoelectronics and Energy & Collaborative Innovation Center of Suzhou Nano Science and Technology, Soochow university, Suzhou* 215006, *China*

[2] *Beijing National Laboratory for Condensed Matter Physics, Institute of Physics, Chinese Academy of Sciences, Beijing* 100190, *China*

[3] *College of Science, Nanjing University of Aeronautics and Astronautics, Nanjing* 211106, *China*

(Received 31 January 2016; revised manuscript received 25 February 2016; published online 5 April 2016)

We present an infrared spectroscopy study of charge dynamics in $CaCo_2As_2$ single crystal. In this material, the optical conductivity can be described by two Drude components with different scattering rates ($1/\tau$): a broad incoherent background and a narrow Drude component. By monitoring the temperature dependence, we find that only the narrow Drude component is temperature-dependent and determines the transport properties. Especially a Fermi liquid behavior of carriers is revealed by the T^2 behavior in the dc resistivity ρ_n and scattering rate $1/\tau_n$, indicating a coherent nature of quasiparticles in the narrow Drude subsystem.

Keywords: infrared spectroscopy, optical conductivity, Fermi liquid

PACS: 72.15.–v, 74.70.–b, 78.30.–j **DOI:** 10.1088/1674-1056/25/5/057201

1. Introduction

Chemical substitution, or doping, is the most common way to tune the properties of a correlated material. In iron-based superconductors (FeSCs), superconductivity is induced by various doping processes into metallic parent compounds. For example, in $BaFe_2As_2$ (122 system), doping with either electrons[1] or holes[2] suppresses the magnetic order, showing superconductivity with a maximum T_c close to the edges of the magnetic dome. The resistivity with different doping levels shows a temperature dependence from T linear to T^2, revealing a crossover from non-Fermi liquid to Fermi liquid.[3–5]

FeSCs are Fe $3d^6$ multi-orbital systems. All the Fe 3d bands (or orbitals) exist near the Fermi level, resulting in complicated hole- and electron-like Fermi surface sheets,[6,7] and each Fe 3d band turns out to have different fillings and bandwidths.[8] In these multi-band systems the electronic correlations are mainly caused by the Hund rule coupling instead of the strong intraband Coulomb interactions as in cuprates.[9,10] Up to now, FeSCs were thought to be in the intermediate correlation regime. Nevertheless, many features, which are usually observed in some strongly correlated materials, were also found in FeSCs,[11,12] such as the linear temperature-dependent resistivity,[3,4] characteristic of a non-Fermi liquid. The non-Fermi-liquid behavior or linear temperature dependence of the resistivity is often taken as the hallmark of a quantum critical regime.[13,14]

It is well known that the electronic correlations in FeSCs are strongly band-dependent. The coexistence of electrons with different electronic correlations (coherent part and incoherent part) could be reflected in the charge excitation spectra which can be measured by the optical spectroscopy technique. In a multi-band environment, the optical conductivity is a sum of the contribution over the bands, and it happens to be parallel of resistances. Indeed, this is the case found by many previous optical studies on FeSCs,[15–19] in which the optical conductivity can be characterized by two Drude terms with different scattering rates; and the total Drude weight is a sum of terms $\sim (n/m^*)_\alpha$, where n is a carrier concentration and m^* is an effective mass, and α is the band index. Thus, in the situation of heavy differentiation of correlation strength, the transport properties are highly influenced by the bands of the weakly correlated ones (or more coherent ones).

Optical spectroscopy is a bulk-sensitive and energy-resolved probe, and it turns out to be a powerful tool to study charge dynamics of the multi-band system. In this paper, we report a detailed optical study on high quality $CaCo_2As_2$ single crystals, a counterpart of the 122 parent compound $CaFe_2As_2$. We found that the optical conductivity of $CaCo_2As_2$ can be decomposed into a narrow Drude (coherent) component and a broad incoherent background. Upon cooling, only the narrow Drude component is temperature-dependent and determines the transport properties. This subsystem re-

*Project supported by the National Basic Research Program of China (Grant Nos. 2012CB821400, 2012CB921302, and 2015CB921303) and the National Natural Science Foundation of China (Grants Nos. 11274237, 91121004, 51228201, and 11004238). Wei Zhang also thanks the support of the Priority Academic Program Development of Jiangsu Higher Education Institutions (PAPD).

†Corresponding author. E-mail: yanghao@nuaa.edu.cn

‡Corresponding author. E-mail: xgqiu@iphy.ac.cn

© 2016 Chinese Physical Society and IOP Publishing Ltd

veals a T^2 behavior in the dc resistivity and scattering rate disclosing a Fermi-liquid behavior in this material.

2. Experiments

High-quality $CaCo_2As_2$ single crystals were grown with the flux method.[20] The *ab*-plane reflectivity $R(\omega)$ was measured at a near-normal angle of incidence on a Bruker VERTEX 80v FTIR spectrometer. An *in situ* gold overfilling technique[21] was used to obtain the absolute reflectivity $R(\omega)$ of the sample. Data from 50 to 15000 cm^{-1} were collected at 13 different temperatures from 300 K to 10 K on a freshly cleaved surface on an ARS–Helitran crysostat. Since a Kramers–Kronig analysis requires a broad spectral range, $R(\omega)$ was extended to the UV range (up to 50000 cm^{-1}) at room temperature with an AvaSpec-2048×14 fiber optic spectrometer.

3. Results and discussion

Figure 1 shows the reflectivity spectra $R(\omega)$ for $CaCo_2As_2$ in the far-infrared region at several temperatures. $R(\omega)$ shows a typical metallic response, having relatively high value and approaching unity at low frequencies. Two sharp features at ~ 180 cm^{-1} and ~ 260 cm^{-1} are associated with the symmetry-allowed *ab* plane infrared-active phonon modes,[22–25] which will not be discussed in this paper. The inset displays the room-temperature $R(\omega)$ up to 15000 cm^{-1} for $CaCo_2As_2$. $R(\omega)$ shows a plasma edge at ~ 6000 cm^{-1}. The plasma edge is larger than the value ~ 2000 cm^{-1} in the typical 122 parent compound $BaFe_2As_2$ (red curve). The large value of the plasma edge generally suggests an increase of carrier density, consistent with the expanded electron Fermi pockets with electron doping in 122 system compounds.[7,26]

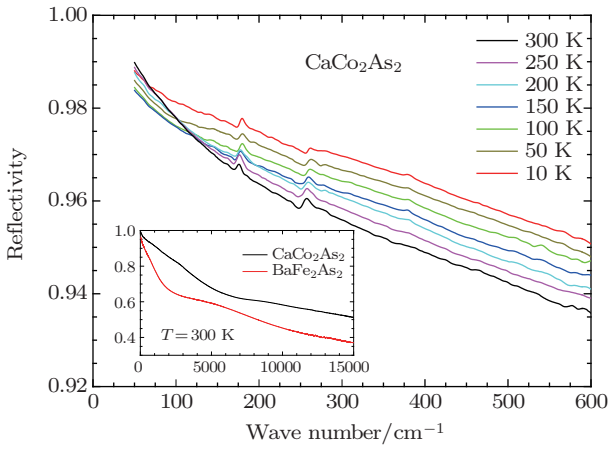


Fig. 1. (color online) Temperature-dependent reflectivity of $CaCo_2As_2$ in the far infrared region. Inset: 300-K reflectivity over a wide frequency range for $CaCo_2As_2$ and $BaFe_2As_2$.

The real part of the optical conductivity $\sigma_1(\omega)$, which provides more direct information about the charge dynamics, has been determined via a Kramers–Kronig analysis of the reflectivity spectra $R(\omega)$.[27] Below the lowest measured frequency, we used a Hagen–Rubens ($R = 1 - A\sqrt{\omega}$) form for the low-frequency extrapolation. Above the highest measured frequency, we assume a constant reflectivity up to 12.5 eV, followed by a free-electron (ω^{-4}) response.

Figure 2 displays the optical conductivity $\sigma_1(\omega)$ at several temperatures between 10 and 300 K in the frequency up to 4000 cm^{-1}. The low-frequency $\sigma_1(\omega)$ has a Drude-like peak centered at zero frequency, indicating the metallic nature of the material. This is consistent with the reflectivity analysis. The width of the Drude peak at half maximum represents the quasiparticle scattering rate, while the area under the Drude peak (spectral weight) is proportional to the free carrier density. As the temperature is reduced, this Drude-like peak narrows with a concomitant increase of the low-frequency optical conductivity. The inset of Fig. 2 shows the 300 K conductivity over a broader spectral range for $CaCo_2As_2$ and $BaFe_2As_2$. In contrast to the small Drude peak in $BaFe_2As_2$, the $CaCo_2As_2$ has a Drude component with significantly larger spectral weight, indicating that the carrier density increases in $CaCo_2As_2$, which is also consistent with the reflectivity analysis. In addition to the Drude-like peak, the optical conductivity of $CaCo_2As_2$ shows a rather flat region with a long tail extending to ~ 4000 cm^{-1} and followed by a temperature-independent mid-infrared peak around 8000 cm^{-1} indicative of strong interband transitions.

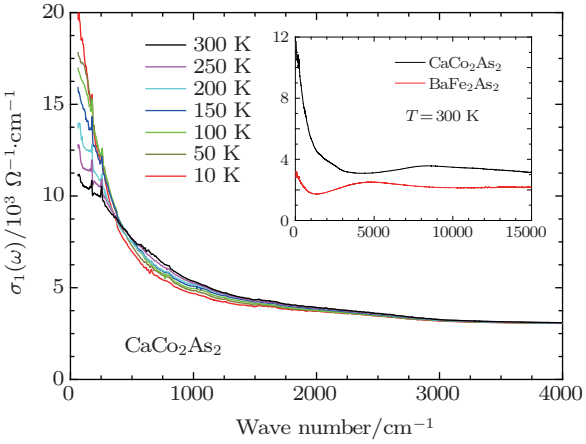


Fig. 2. (color online) The real part of the optical conductivity at different temperatures for $CaCo_2As_2$ up to 4000 cm^{-1}. Inset: 300-K optical conductivity over a wide frequency range for $CaCo_2As_2$ and $BaFe_2As_2$.

The optical conductivity is conveniently parameterized by a Drude–Lorentz model

$$\sigma_1(\omega) = \frac{2\pi}{Z_0}\left[\sum_j \frac{\Omega_{p,j}^2}{\omega^2\tau_j + \frac{1}{\tau_j}} + \sum_k \frac{\gamma_k\omega^2 S_k^2}{(\Omega_k^2 - \omega^2)^2 + \gamma_k^2\omega^2}\right], \quad (1)$$

where Z_0 is the vacuum impedance. The first term in Eq. (1) corresponds to the Drude response characterized by a plasma frequency $\Omega_{p,j}$ and a scattering rate $1/\tau_j$. The second term is a

sum of Lorentz oscillators, each having a resonance frequency Ω_k, a line width γ_k, and a weight S_k. The Drude term accounts for the free carrier response, while the Lorentz contributions represent bound excitations.

In the previous works on pnictides,[15–19] the optical conductivity $\sigma_1(\omega)$ can be modeled reasonably by the superposition of two Drude components and series of Lorentz terms over a wide frequency range. As shown in Fig. 3(a), we employed a similar fit for $CaCo_2As_2$ at 150 K. It is noted that the low frequency $\sigma_1(\omega)$ is characterized by a coherent narrow Drude (blue line) with a small scattering rate ($1/\tau_n \sim 314$ cm^{-1}) and an incoherent broad Drude (magenta line) with a large scattering rate ($1/\tau_b \sim 3474$ cm^{-1}), as well as two Lorentzian oscillators at higher frequencies corresponds to the interband excitation in the mid-infrared region. The fitting parameters at 150 K are summarized in Table 1.

Table 1. The Drude–Lorentz fitting results of the optical conductivity at 150 K, where $\Omega_{p,j}$ and τ_j are the plasma frequency and scattering rate for the jth Drude component (Dj), and Ω_k, S_k, and γ are the oscillator frequency, strength, and line width of the kth Lorentz mode (L_k). All units are in cm^{-1}.

Type	Ω_k	$1/\tau_j, \gamma$	$\Omega_{p,j}, S_k$
D1	–	314	14963
D2	–	3474	29853
L1	9620	16190	50720
L2	521703	8450130	1542799

The temperature dependence of the two Drude components provides information about the nature of the two different types of carriers in this material. As shown in Fig. 2, for all data at different temperatures, the long flat tail of $\sigma_1(\omega)$ changes very slightly with temperature, meaning that it just contributes a constant background on the optical conductivity. The temperature-independent part of $\sigma_1(\omega)$ is indicated by the light-gray shaded area in Fig. 3(a), and it consists of the broad Drude component σ_b (magenta hatched area) and two oscillators that associate with the high-frequency contributions (orange and dark-yellow hatched area). On the top of the constant background, the remaining temperature-dependent contribution is the narrow Drude component $\sigma_n(\omega)$

$$\sigma_n(\omega) = \frac{2\pi}{Z_0}\frac{\Omega_{p,n}^2}{\omega^2\tau_n + \frac{1}{\tau_n}}. \quad (2)$$

Upon cooling, the scattering rate $1/\tau_n$ becomes narrowing, while the plasma frequency $\Omega_{p,n}$ is roughly a constant, indicating that there seems to be no considerable transfer of spectral weight between both Drude subsystems. As shown in Table 1, the coherent narrow component σ_n contains only about 1/4 of the spectral weight compared to the incoherent background σ_b, but it turns out that it is of superior importance to low-frequency properties and transport properties.

The two Drude terms' contributions to the total dc resistivity can be considered as a parallel circuit

$$\sigma_{total}(T) = \sigma_n(T) + \sigma_b. \quad (3)$$

In order to reveal the temperature dependence of the subsystem described by σ_n, we simply subtract the temperature-independent part σ_b by the Drude–Lorentz fits. As shown by the thin lines through the corresponding data in Fig. 3(b), the temperature-dependent part of $\sigma_1(\omega)$ can be described well with the single narrow Drude component $\sigma_n(\omega)$.

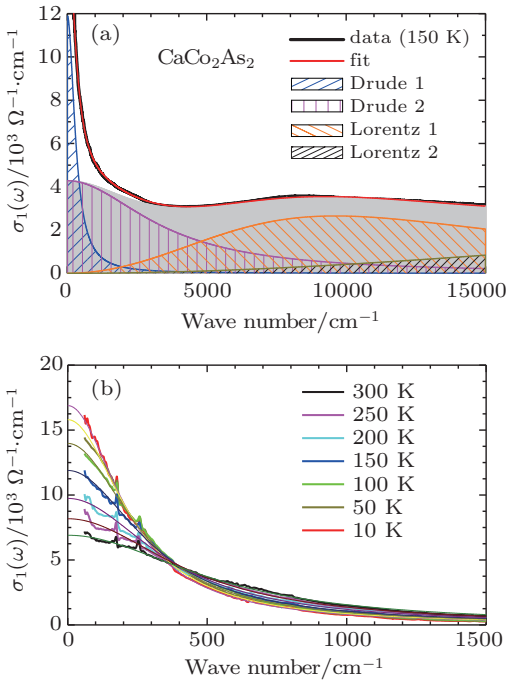


Fig. 3. (color online) (a) The measured $\sigma_1(\omega)$ at 150 K (thick black line) in a wide spectral range for $CaCo_2As_2$, fitting with the Drude–Lorentz model (thin red line). The optical conductivity of $CaCo_2As_2$ can be separated into temperature-dependent and -independent parts. The temperature-independent part consists from the incoherent broad Drude term σ_b (magenta line), and two Lorentzian oscillators at higher frequencies (orange and dark yellow lines). The sum of the three contributions results in the light gray shaded area. The unshaded area below the curves is temperature dependent and can be described by a single Drude term σ_n (blue line). Temperature evolution of σ_n for $CaCo_2As_2$ is shown in panel (b). The thin lines through the data are fits with a single Drude term.

Figures 4(a) and 4(b) display the temperature dependence of dc resistivity $\rho_n(T) = 1/\sigma_n(\omega \to 0)$ and scattering rate $1/\tau_n$. Across all the measured temperature range, ρ_n and $1/\tau_n$ present a T^2-dependent behavior. This T^2 temperature dependence is expected for electron–electron scattering that is supposed to be dominant for correlated electron systems at low temperatures and subject to Landau's theory of a Fermi liquid. The Fermi liquid behavior revealed by the T^2 dependence of the scattering rate and dc resistivity in $CaCo_2As_2$ indicates a coherent nature of quasiparticles in the narrow Drude subsystem.

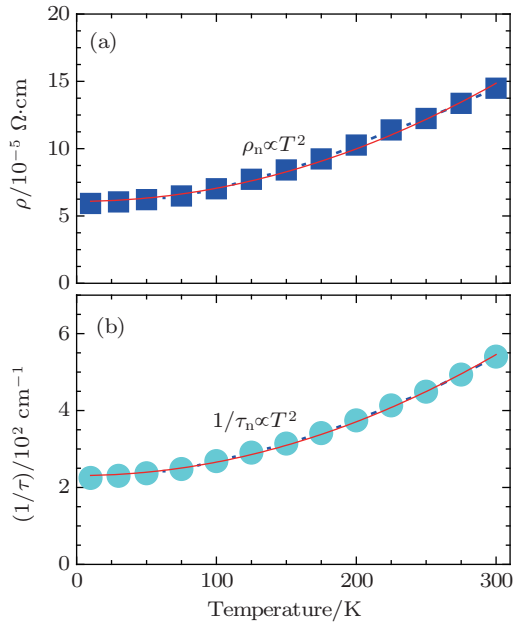


Fig. 4. (color online) The temperature dependence of the fitting parameters for the Narrow Drude term in $CaCo_2As_2$: (a) the reverse dc conductivity $\rho = 1/\sigma_1(\omega \to 0)$ and (b) the scattering rate $1/\tau$, respectively. The red lines in panels (a) and (b) are the T^2 fits.

4. Conclusion

In summary, we have measured the electrodynamics properties of $CaCo_2As_2$ single crystal in a wide frequency range as a function of temperature. The optical conductivity of $CaCo_2As_2$ can be decomposed into a broad temperature-independent background and a narrow Drude-type component which solely determines the transport properties. The narrow Drude subsystem reveals a T^2 behavior in the dc resistivity and scattering rate up to room temperature, indicating a Fermi-liquid behavior in this material.

References

[1] Ni N, Tillman M E, Yan J Q, Kracher A, Hannahs S T, Bud'ko S L and Canfield P C 2008 *Phys. Rev. B* **78** 214515
[2] Rotter M, Tegel M and Johrendt D 2008 *Phys. Rev. Lett.* **101** 107006
[3] Doiron-Leyraud N, Auban-Senzier P, René de Cotret S, Bourbonnais C, Jérome D, Bechgaard K and Taillefer L 2009 *Phys. Rev. B* **80** 214531
[4] Kasahara S, Shibauchi T, Hashimoto K, Ikada K, Tokeya H, Hirata K, Terashima T and Matsuda Y 2010 *Phys. Rev. B* **81** 184519
[5] Dai Y M, Miao H, Xing L Y, Wang X C, Wang P S, Xiao H, Qian T, Richard P, Qiu X G, Yu W, Jin C Q, Wang Z, Johnson P D, Homes C C and Ding H 2015 *Phys. Rev. X* **5** 031035
[6] Ding H, Richard P, Nakayama K, Sugawara K, Arakane T, Sekiba Y, Takayama A, Souma S, Sato T, Takahashi T, Wang Z, Dai X, Fang Z, Chen G F, Luo J L and Wang N L 2008 *Europhys. Lett.* **83** 47001
[7] Malaeb W, Yoshida T, Fujimori A, Kubota M, Ono K, Kihou K, Shirage P M, Kito H, Iyo A, Eisaki H, Nakajima Y, Tamegai T and Arita R 2009 *JPSJ* **78** 123706
[8] Lu D H, Yi M, Mo S K, Erickson A S, Analytis J, Chu J H, Singh D J, Hussain Z, Geballe T H, Fisher I R and Shen Z X 2008 *Nature* **455** 81
[9] Yin Z P, Haule K and Kotliar G 2011 *Nat. Mater.* **10** 932
[10] Misawa T, Nakamura K and Imada M 2012 *Phys. Rev. Lett.* **108** 177007
[11] Mazin I I 2010 *Nature* **464** 183
[12] Johnston D C 2010 *Adv. Phys.* **59** 803
[13] Hashimoto K, Cho K, Shibauchi T, Kasahara S, Mizukami Y, Katsumata R, Tsuruhara Y, Terashima T, Ikeda H, Tanatar M A, Kitano H, Salovich N, Giannetta R W, Walmsley P, Carrington A, Prozorov R and Matsuda Y 2012 *Science* **336** 1554
[14] Walmsley P, Putzke C, Malone L, Guillamón I, Vignolles D, Proust C, Badoux S, Coldea A I, Watson M D, Kasahara S, Mizukami Y, Shibauchi T, Matsuda Y and Carrington A 2013 *Phys. Rev. Lett.* **110** 257002
[15] Wu D, Barisic N, Kallina P, Faridian A, Gorshunov B, Drichko N, Li L J, Lin X, Cao G H, Xu Z A, Wang N L and Dressel M 2010 *Phys. Rev. B* **81** 100512
[16] Tu J J, Li J, Liu W, Punnoose A, Gong Y, Ren Y H, Li L J, Cao G H, Xu Z A and Homes C C 2010 *Phys. Rev. B* **82** 174509
[17] Nakajima M, Ishida S, Kihou K, Tomioka Y, Ito T, Yoshida Y, Lee C H, Kito H, Iyo A, Eisaki H, Kojima K M and Uchida S 2010 *Phys. Rev. B* **81** 104528
[18] Dai Y M, Xu B, Shen B, Xiao H, Wen H H, Qiu X G, Homes C C and Lobo R P S M 2013 *Phys. Rev. Lett.* **111** 117001
[19] Yang Y X, Xiong R, Fang Z H, Xu B, Xiao H, Qiu X G, Shi J and Wang K 2014 *Chin. Phys. B* **23** 107401
[20] Zhang W, Nadeem K, Xiao H, Yang R, Xu B, Yang H and Qiu X G 2015 *Phys. Rev. B* **92** 144416
[21] Homes C C, Reedyk M, Cradles D A and Timusk T 1993 *Appl. Opt.* **32** 2976
[22] Akrap A, Tu J J, Li L J, Cao G H, Xu Z A and Homes C C 2009 *Phys. Rev. B* **80** 180502
[23] Schafgans A A, Pursley B C, LaForge A D, Sefat A S, Mandrus D and Basov D N 2011 *Phys. Rev. B* **84** 052501
[24] Dai Y M, Xu B, Shen B, Xiao H, Lobo R P S M and Qiu X G 2012 *Chin. Phys. B* **21** 077403
[25] Xu B, Dai Y M, Shen B, Xiao H, Ye Z R, Forget A, Colson D, Feng D L, Wen H H, Homes C C, Qiu X G and Lobo R P S M 2015 *Phys. Rev. B* **92** 104510
[26] Sekiba Y, Sato T, Nakayama K, Terashima K, Richard P, Bowen J H, Ding H, Xu Y M, Li L J, Cao G H, Xu Z A and Takahashi T 2009 *New J. Phys.* **11** 025020
[27] Dressel M and Grüner G 2002 *Electrodynamics of Solids* (Cambridge: Cambridge University Press)